Multi-criteria optimization of pitch curves for screw-type vacuum pumps

Dipl.-Ing. **D. Pfaller,** Prof. Dr.-Ing. **A. Brümmer**, Prof. Dr.-Ing. **K. Kauder**
Fachgebiet Fluidtechnik, Technische Universität Dortmund, Germany [1]

Abstract

The present article on the energetic optimization of dry-running screw-type vacuum pumps deals with the design of pitch curves for screw-type vacuum pumps. An analysis is made, in particular, on the theoretical power demand. For the development of the computation model, the high number of working chambers on the rotors of the screw spindle is reproduced by means of a series connection of individual pump stages. The volumes of the chambers are varied at constant overall chamber volume of the screw-type vacuum pump. The dissipative gap mass flows arising due to pressure differences between the working chambers are represented by means of a lossy gap flow. With regard to a minimal specific internal work, a pitch curve turns out to be optimal when it deviates from the current designs of screw-type vacuum pumps, in particular in the central rotor section.

1 Introduction

At the chair of fluidics, the design possibilities of screw-type vacuum pumps are surveyed within the framework of a research project supported by the German Research Foundation (DFG). The research project is aimed at the development of a method for the energetic design of dry-running screw-type vacuum pumps. In practice, the screw-type vacuum pump is characterized, above all, by its high achievable pressure ratio, the high suction capacity and the possibility to be operated in a “dry”-running mode [1].

The large suction-pressure range, reaching from low to fine vacuum, represents a challenge for the thermodynamic description of the compression process. In addition to the high achievable pressure ratios of more than one million and the resulting gas temperatures, also the different forms of flow, from continuum to molecular flow, complicate the analytical description of flow processes inside the pump.

The first spindle pumps on the market showed a constant pitch and were characterized by an “isochoric“ transport phase [2]. From an energetic point of view, however, a compression of the working gas is desirable, so that pumps with internal compression were developed [3]. A possibility to reduce the volume of the working chamber prior to its opening towards the pressure side would be the design of a discharge contour in the housing. This decelerates

[1)] **This work is kindly supported by the Deutsche Forschungsgemeinschaft (DFG)**

the opening of the working chamber by a defined rotation angle and thus generates the compression of the enclosed working gas. Another possibility would be the modification of the working chamber geometry during the conveying phase. For this purpose, either the pitch along the rotor axis is changed or the ratio of rotor head diameter and root diameter. Both methods result in a variation of the working chamber volume along the rotor axis.

Here, the question arises of how should the pitch curve of the working chamber volume for a given pressure ratio along the rotor axis be designed to achieve an energetically favourable operating behaviour. Apart from the pressure ratio of the adjoining working chambers, also the gap mass flow is important for the design of the pitch.

A simple model calculation shall illustrate the influence of the gap mass flow on the discharge mass flow of the stages. A screw-type vacuum pump with a suction pressure of 100 Pa and a suction capacity of 200 $m^3 \cdot h^{-1}$ delivers a mass flow of approx. $7 \cdot 10^{-5}$ $kg \cdot s^{-1}$. The gap mass flow for a gap in the area of the high-pressure side (HP), known from various calculations [4], is at about 0.02 $kg \cdot s^{-1}$. In this example, the discharge mass flow of the vacuum pump accounts for only 0.3% of the discharge mass flow of the stage at the pressure side.

The model calculation shows that the pitch design of the working chamber volume analogous to the multi-stage compressor structure, where a constant pressure ratio is applied to the individual stages, is not effective in case of the screw-type vacuum pump.

2 Model concept and calculation bases

The rotor of a screw spindle for the application as vacuum pump is characterized by a high wrap angle, **Fig.1**. This also results in a high number of working chambers between suction and pressure side. The high number of working chambers along the rotor axis leads to the assumption that the pressure distribution within the screw-type vacuum pump can be calculated using the conservation of mass principles and thus enables both information about the attainable final pressure and the suction capacity at determined suction pressures. The thermal influences on the operational behaviour of a screw-type vacuum pump with the usual very high pressure ratios are not be neglected in steady-state operation, but closely related to the calculation of the gas temperatures arising from thermal stress as well as to the heat transfer and to the cooling of the components.

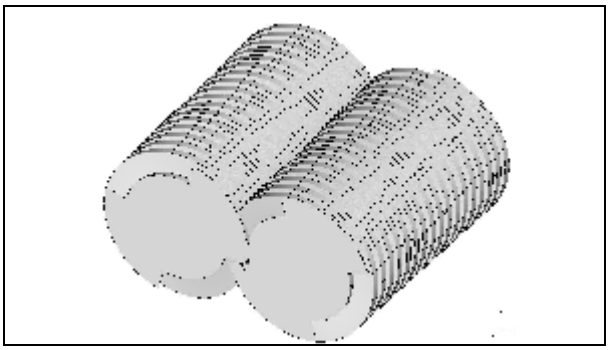

Fig. 1 Pair of rotors of a screw-type vacuum pump

Despite approaches which include an integral calculation of the heat balance of a screw-type vacuum pump [5], the heat transfer conditions in vacuum have not yet been fully researched.

However, in order to enable the provision of verifiable information on the operating characteristics of the screw-type vacuum pump, a “cold“ – thus thermally undeformed – machine is assumed below. This idealized state can be simulated in test operation by short measuring cycles at the cold machine and can thus be verified.

For the calculation of chamber pressures and mass flows, the closed working chambers of the screw spindle are connected by pump stages (**Fig 2**). In this case, the discharge volume flow $\dot{V}_{C,i}$ of stage *i* results from the working chamber volume $V_{C,i}$ and the rotational speed *n*. In combination with suction pressure $p_{C,i}$ and gas temperature $T_{C,i}$ prior to stage *i*, this results in a discharge mass flow $\dot{m}_{C,i}$ of stage *i*.

The local gap mass flow $\dot{m}_{G,i}$ of the i-th stage results from the respective gap area $A_{G,i}$ and the given pressure ratio $\Pi_i = \frac{p_{i+1}}{p_i}$ over the gap of stage i for subcritical pressure ratios $\Pi_i^{-1} < 0.528(Air)$ to

$$\dot{m}_{G,i} = a_{G,i} \cdot A_{G,i} \cdot \left(\Pi_i\right)^{-\frac{1}{k}} \cdot \frac{p_{C,i+1}}{R \cdot T_{C,i+1}} \cdot \sqrt{\frac{2 \cdot k}{k-1} \cdot R \cdot T_{C,i+1}\left(1-\left(\Pi_i\right)^{\frac{1-k}{k}}\right)}$$

and for supercritical pressure ratios $\Pi_i^{-1} > 0.528(Air)$ to

$$\dot{m}_{G,i} = a_{G,i} \cdot A_{G,i} \cdot \left(\frac{2}{k+1}\right) \cdot \frac{p_{C,i+1}}{R \cdot T_{C,i+1}} \cdot \sqrt{\frac{2 \cdot k}{k+1} \cdot R \cdot T_{C,i+1}} \,.$$

For a steady-state operating point with defined suction capacity and/or discharge mass flow, the discharged mass flow $\dot{m}_{LP} = \dot{m}_{HP}$ is added to the local gap mass flow $\dot{m}_{G,i}$ of the individual stage resulting in a discharge mass flow $\dot{m}_{C,i}$ of the respective stage $\dot{m}_{C,i} = \dot{m}_{G,i} + \dot{m}_{HP}$.

For steady-state final pressure operation, the local discharge mass flow of each stage $\dot{m}_{C,i}$ must correspond to the local gap mass flow $\dot{m}_{G,i}$.

The control factor in the calculation of mass flows is the pressure in the working chambers $p_{c,i}$. The calculation of the internal specific work per stage w_i occurs on the assumption of an isentropic compression process for the working medium air which is regarded as ideal gas.

$$w_i = c_p \cdot T_{C,i}\left(\Pi_i^{\frac{k-1}{k}} - 1\right)$$

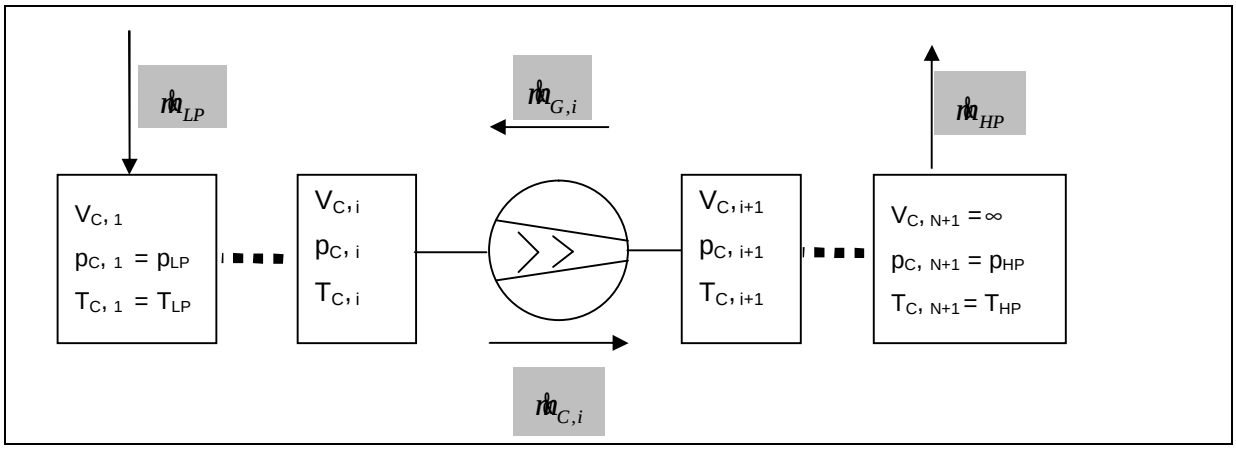

Fig. 2: Abstraction of the spindle into a series connection of working chambers and stages with gap and discharge mass flow of the individual stage

$i \in [1, N]$ *Stage index*

$V_{C,i}$ *Working chamber volume*

$p_{C,I}$ *Pressure prior to stage i*

$T_{C,i}$ *Temperature prior to stage i*

$\dot{m}_{C,i}$ *Conveying mass flow over stage i*

$\dot{m}_{G,i}$ Gap mass flow over stage i

$\dot{m}_{HP}$ Mass flow through HP-port

$\dot{m}_{LP}$ *Mass flow through LP-port*

The multiplication of the respective discharge mass flow $\dot{m}_{C,i}$ of stage i results in the internal power P_i of stage *i*. The internal power of the series-connected pump stages P_{tot} can be determined by the addition of the individual stage powers

$$P_{tot} = \sum_{i=1}^{N} P_i = \sum_{i=1}^{N} w_i \cdot \dot{m}_{C,i} .$$

Since neither the heat transfer conditions within the working chambers nor the mutual influence of the energy transported via gap mass flows are covered, the simplified approach of complete re-cooling of the air in the chambers between the stages is chosen. For the purpose of comparative calculations however, a re-cooling rate per chamber can be applied to the model.

The basic concept of the calculation approach goes back to an article on screw machines written by K. Kauder and A. Rohe [6]. The adopted approach will be expanded by the gap connections of the blow hole, the profile gap and the radial gap.

3 Simplified model calculation for a two-stage screw-type vacuum pump

In order to illustrate the influences of the modelling, a two-stage compression is detailed in the first step. Here, optimization regarding the specific internal work w_{ges} is carried out. For

calculation purposes, the complex gap situation in the spindle is simplified in order to ensure the traceability of the calculation steps. A lossy gap connection, with dimension and connected chambers corresponding to the housing gap, is added to each pump stage. Gap connections corresponding to a connection between two working chambers which are not directly series-arranged in discharge direction are not taken into account in this model calculation.

The gap areas $A_{G,i} = A_G$ = const. as well as the operating parameters are constant for all stages. Within the framework of the simplified approach, the orifice coefficients $\alpha_{G,i} = \alpha_G$ = const. of the gap are held constant. Thus, the internal power of the screw spindle only depends on the stage pressure ratios and the discharged mass flow $\dot{m}_{HP}$.

The modelling is based on a constant total volume of the working chambers

$$V_{tot} = \sum_{i=1}^{n} V_{C,i} = const..$$

This approach corresponds to the assumption of a constant rotor length and scoop area for the screw-type vacuum pump. Subsequently, the energetically optimal allocation of the constant total volume to the available working chambers – i.e. to the working chambers $V_{C,1}$ and $V_{C,2}$ of the example - is searched for.

With real rotor geometry, the variation of the working chamber volume per stage corresponds to a variation in the pitch between the working chambers at constant rotor length. For the purpose of the model calculation, all other geometry and operating parameters are held constant, see **Table 1.**

Table 1: Parameters for the calculation of a two-stage vacuum pump

Specific heat capacity c_p	1005 J ·kg^{-1}·K^{-1}
Gas temperature $T_{LP} = T_{HP}$	293 K
Gas constant R	287 J·kg^{-1}·K^{-1}
Gap area A_G	1.66·10^{-4} m^2
Orifice coefficient α_G	0,8
Total volume of working chambers V_{tot}	1.4·10^{-3} m^3
Discharge pressure p_{HP}	10^5 Pa
Rotational speed n	5000 min^{-1}

Thus, for the calculation of the pressure distribution and the discharge mass flow of the screw-type vacuum pump an equation system of one equation per stage results.

Therefore, suction and discharge pressure (here in general 10^5 Pa) as well as the intake temperature and rotational speed of the screw-type vacuum pump are predetermined. For the example of a two-stage screw-type vacuum pump, pressure $p_{C,2}$ and discharge mass flow $\dot{m}_{HP}$ for variably determined chamber volumes $V_{C,i}$ and $V_{C,2}$ at constant total chamber volume V_{tot} are determined by iteration. From the

subsequently gathered values for pressures and pressure ratios, the internal powers per stage as well as the internal power of the screw-type vacuum pump result.

Apart from the internal power, the specific internal work w_{tot} is of particular interest for the energetic design. Since due to the variable allocation of the total volume, the working chamber volume on the suction side varies, the theoretical discharge mass flow is also variable even at constant suction pressure. The calculated specific works of the screw-type vacuum pump for different ratios of the working chamber volumes are shown in **Fig. 3.**

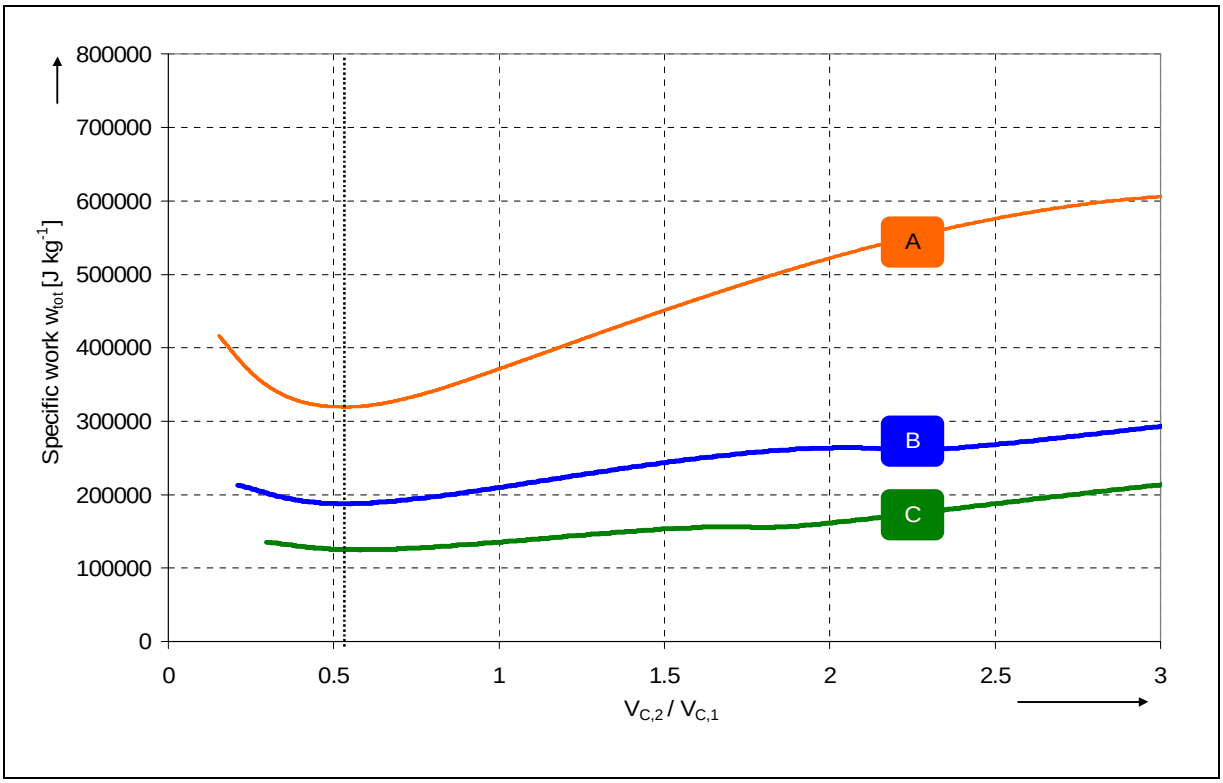

Fig. 3 Curve of the specific work w_{tot} for two-stage compression with variation of the volume ratio between the first and second working chamber at a constant total volume of the working chambers and different suction pressures
A: 20000 Pa (200 mbar), **B**: 30000 Pa (300 mbar), **C**: 40000 Pa (400 mbar)

At first, the calculated specific work w_{tot} shows a decline with the increasing volume ratio of the working chambers $V_{C,2}/V_{C,1}$. At a ratio of the working chamber volumes of approx. $V_{C,2}/V_{C,1} = 0.54$, a minimum of specific work is achieved at the studied suction pressures, see **Table 2**. The ratio increases to 0.58 only at a suction pressure of 40000 Pa.

The major influencing factor for achieving these minimal values in the specific total work w_{tot} is, apart from the discharge mass flow $\dot{m}_{LP} = \dot{m}_{HP}$, the total amount of the power per stage $P_{C,i}$ for the two stages considered. The power $P_{C,i}$ of a stage is calculated from the applied stage compression Π_i and the discharged mass flow of the stage $\dot{m}_{C,i}$. In a first approximation, the stage pressure ratios vary analogously to the chamber volumes.

Table 2: Parameters for the position of the specific work minima for different suction pressures

p_{LP} [Pa]	20000	30000	40000
$\dot{m}_{HP}$ [kg·s^{-1}]	0.021	0.035	0.049
$\dot{m}_{C,1}$ [kg·s^{-1}]	0.037	0.056	0.072
$\dot{m}_{C,2}$ [kg·s^{-1}]	0.052	0.065	0.077
Π_1	2.62	2.19	1.84
Π_2	1.91	1.52	1.36
$\frac{\Pi_2}{\Pi_1}$	0.73	0.69	0.74
$\frac{V_{C,2}}{V_{C,1}}$	0.54	0.54	0.58
$\frac{P_2}{P_1}$	0.89	0.59	0.51
P_{tot} [W]	6580	6575	6127
$w_{tot} = \frac{P_{tot}}{\dot{m}_{HP}} \left[\frac{\mathrm{J}}{\mathrm{kg}}\right]$	313333	187857	125041

The gap mass flow $\dot{m}_{G,i}$ relevant for the respective discharge mass flow per stage $\dot{m}_{C,i}$ depends both on the stage pressure ratio and on the density of the gas when flowing into the gap. With increasing chamber size, the stage pressure ratio increases and, consequently, also the ratio of the gap mass flows. Once the critical pressure ratio over the gap is reached, the gap mass flow depends only on the density of the working gas at the gap inlet. Thus, the internal work $w_{C,1}$ of the first stage increases with the decreasing volume ratio $V_{C,2}/V_{C,1}$, and the internal work of the second stage $w_{C,2}$ decreases analogously to the increasing pressure ratio of the stage. Under said boundary conditions and for a suction pressure of 20000 Pa the minimal totalized power P_{tot} is attained at a volume ratio $V_{C,2}/V_{C,1}$ of 0.73.

The discharge mass flow $\dot{m}_{LP} = \dot{m}_{HP}$ results from the volume of the sucking working chamber $V_{C,1}$ and the returning gap mass flow $\dot{m}_{G,1}$. At small volume ratios $V_{C,2}/V_{C,1}$, the size of the sucking working chamber and thus the theoretical discharge mass flow are maximal. Due to the small working chamber on the suction side, the stage pressure ratio Π_1 of the sucking working chamber corresponds nearly to the total pressure ratio Π_{ges} or can even exceed it in case of extreme values. For the volume ratio, the returning mass flow $\dot{m}_{G,1}$ is maximal and reduces the mass flow $\dot{m}_{HP}$ sucked from the low-pressure range. Due to the reduction of the sucking stage, an increase in the volume ratio of the working chamber $V_{C,2}/V_{C,1}$ results in a reduction of the theoretical discharge mass flow, but due to the lower stage pressure ratio Π_1 and the reduced working gas density between the two stages, also to the reduction of the gap mass flow $\dot{m}_{G,1}$. Because of the countervailing influences, the discharge mass flow $\dot{m}_{HP}$ reaches its maximum value for a suction pressure of 20000 Pa at a volume ratio $V_{C,2}/V_{C,1}$ of about 0.5.

The combination of the discharged mass flow $\dot{m}_{HP}$ and the total amount of internal works of both stages results in the minimum of specific work for the described suction pressure of 20000 Pa at a volume ratio $V_{C,2}/V_{C,1}$ of about 0.54.

Table 2 shows a comparison of the position of specific work minima w_{tot} for different suction pressures.

The pump variation with the highest suction pressure examined does no longer show blocking of the gap flows. In the two variants with low suction pressure, a blocking of the gap mass flow occurs in the stage on the low-pressure side. The ratio of both stage pressure ratio and absolute stage power is below 1. Accordingly, in both cases, a higher value for pressure ratio and internal work is attained in the stage on the low pressure side.

4 Calculation of optimized pitch curves for N-stage screw-type vacuum pumps

Upon completion of the first analyse of a two-stage screw-type vacuum pump, the next step shall be the transition to the realistically designed spindle geometry. This requires the expansion of the number of stages and the modelling of further gap connections. Furthermore, the modelling of the gap connections comprises the housing, which connects two directly successive working chambers on a rotor, the profile gap, which connects two working chambers of the studied two-teeth spindle that are not directly successive in direction of the pressure drop, and the radial gap which reflects a connection to the working chambers on the counter rotor (**Fig. 4**) [4].

In order to cover the different gap flows in the pressure range of the vacuum, the orifice coefficient for the gap connections is calculated from an experimentally determined data base [6] both in dependence of pressure and geometry. Due to the stage numbers of N = 5-12 stages common on the market, which shall also be applied in the simulation, it is no longer possible to calculate all pumps upon a corresponding variation of the chamber volumes $V_{C,i}$ at constant total chamber volume within a reasonable time frame, since the number of pump variants increases exponentially with the number of stages. However, in order to find a pitch curve with the highest possible resolution which indicates the optimum power, evolutionary algorithms are applied. Here, the evolutionary approaches are based on the principles of inheritance and mutation [7]. The pump synthesis occurs in freely selectable group sizes. Afterwards, the pressure profile and the specific work and/or total power for all members of the group are determined (fitness function). In case of screw-type vacuum pumps, a basic distinction must be made between final pressure operation and the operation with discharge mass flow. For the evaluation of the quality of a pump variant in the field of final pressure operation, the final pressure attained and the total power input are used. Within the framework of the article, however, only the operation with discharge mass flow

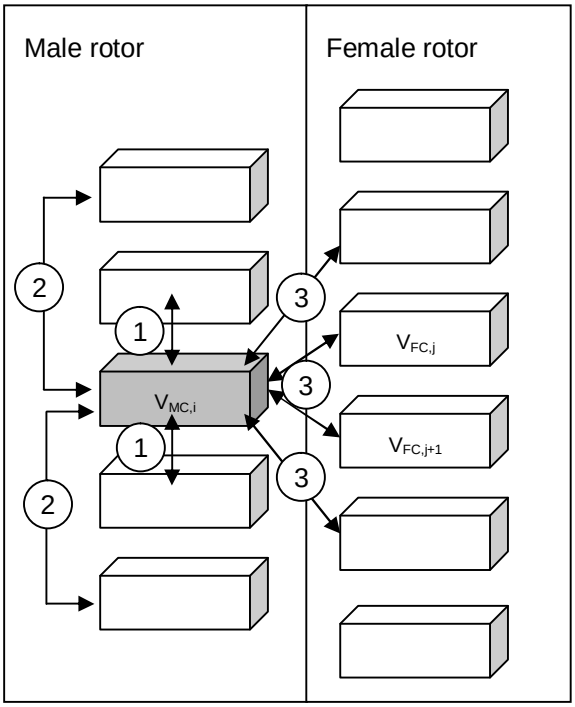

Fig. 4: Chamber model with a two-thread screw-type vacuum pump [4]
1: Housing gap
2: Radial gap
3: Profile gap

shall be analyzed. Here - analogously to the model calculation - a fixed intake pressure and counter pressure are determined for the optimization. Another necessary parameter in

addition to the gap geometry is the rotor speed, which are also predetermined. In contrast to the final pressure operation, the total power related to the discharged mass flow is used as evaluation criterion, thus the specific internal work w_{tot} of the whole screw-type vacuum pump.

Table 4 shows the comparison between the integral values for an 8-stage rotor with a pitch curve optimized with regard to the specific internal work (**Fig. 5)**, a rotor with a linear pitch variation and, as reference, a rotor with constant pitch. For this calculation, the boundary conditions given in **Table 3** were predetermined.

Table 3: Parameters for the calculation of a 8-stage screw type vacuum pump

Gas constant R	287 $J \cdot kg^{-1} \cdot K^{-1}$
Specific heat capacity c_p	1005 $J \cdot kg^{-1} \cdot K^{-1}$
Gas temperature $T_{LP} = T_{HP}$	293 K
Total volume of working chambers	0.0031 m^3
Discharge pressure p_{HP}	10^5 Pa (1 bar)
Suction pressure p_{LP}	100 Pa (1 mbar)
Rotational speed n	5000 min^{-1}

The comparison of the specific work shows clearly that the evolutionary calculation of the pitch causes a significant reduction of the specific internal work. In comparison, however the discharge mass flow and thus the suction capacity of the optimized rotor increase, which causes a slight increase in the total power. Fig. 5 shows the related pitch curve of the optimized rotor after 100 evolution steps.

Table 4: Comparison of the integral values for different pitch curves for boundary conditions according to Table 3.

Spindle type	P_{tot} [W]	$\dot{m}_{HP}$ [kg s^{-1}]	w_{tot} [J/kg]	$\dot{V}_{tot}$ [m^3 s^{-1}]
Constant pitch s = 30mm ($v_{i,tot}$ =1)	4752	$7.3 \cdot 10^{-5}$	$6.5 \cdot 10^{7}$	$6.1 \cdot 10^{-2}$
Linear pitch ($v_{i,tot}$ = 2.7)	3841	$7.2 \cdot 10^{-5}$	$5.4 \cdot 10^{7}$	$6.0 \cdot 10^{-2}$
Optimized pitch ($v_{i,tot}$ = 2.4)	4316	$15 \cdot 10^{-5}$	$3.0 \cdot 10^{7}$	$12 \cdot 10^{-2}$

As expected, the pitch on the LP-side is at first high. The decline in the pitch is followed by an increase in the pitch in the centre of the rotor. Then, at the transition to the working chamber on the pressure side, the pitch declines again.

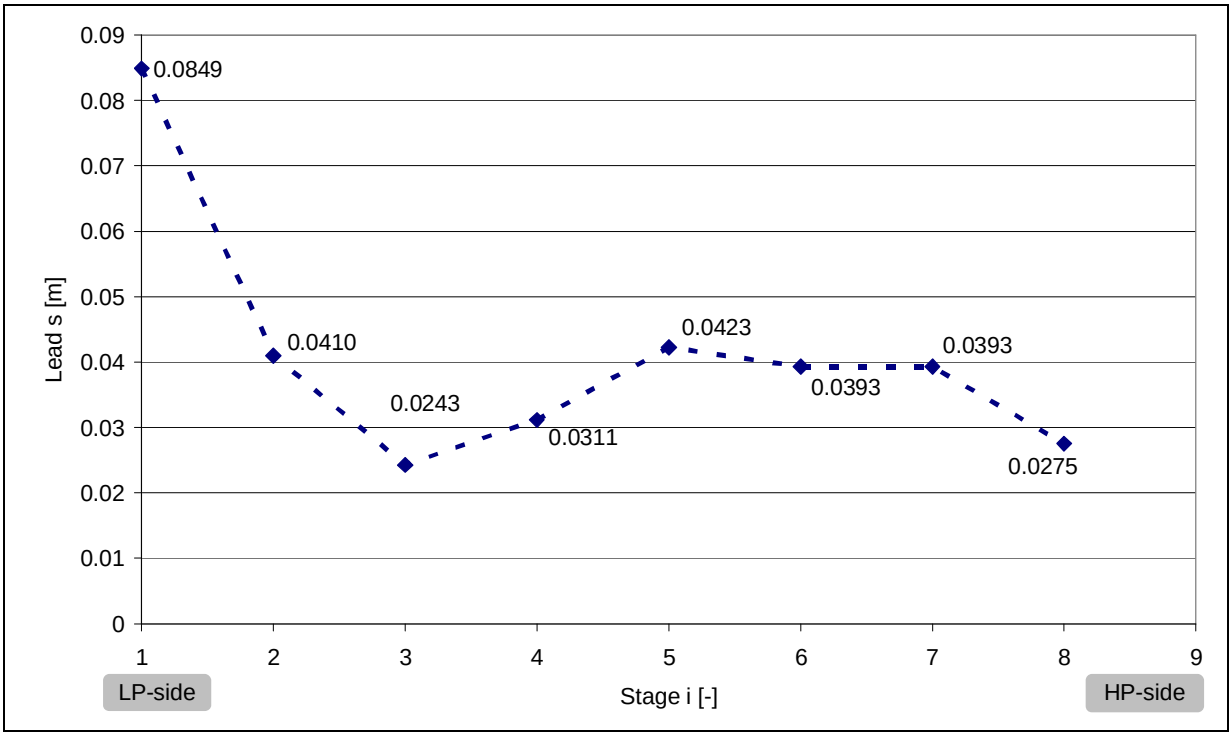

Fig. 5 Pitch curve of the 8-stage rotor optimized with regard to the specific internal work by means of evolutionary algorithms

For the analysis of the pitch curve, the stage pressure ratio P_i and the stage mass flow $\dot{m}_{C,i}$ for the stages $i \in [1,8]$ of the optimized rotor are shown in **Fig. 6**. The stage pressure ratio between all stages is greater than one and reaches a maximum value of four in the area of the LP-side. A reversal of the pressure ratio through the increase in the pitch in the central rotor section does not exist. The curve of the stage pressure ratio qualitatively reflects the pitch curve (Fig. 5). The discharge mass flow per stage increases analogously to the pressure from the suction to the pressure side. The optimized rotor geometry shown attains a discharge mass flow of 0.00015 kg s^{-1}. A comparison with the discharge mass flows of the stages given in **Fig. 7** confirms that the working chambers near the pressure side are mainly filled by returning gap mass flows.

The optimization of the rotor results from the countervailing curves of the stage pressure ratio and the discharge mass flow of the stages. Thus, at the suction side, the stage pressure ratio is maximal and a high specific work is reached, however, due to the low density of the working gas in the suction side area, the conveyed mass flow made up of gap flow and discharge mass flow is low. The absolute power of the stage is therefore low, despite the high stage pressure ratio. In the next stage, the stage pressure ratio decreases, and the specific work decreases accordingly.

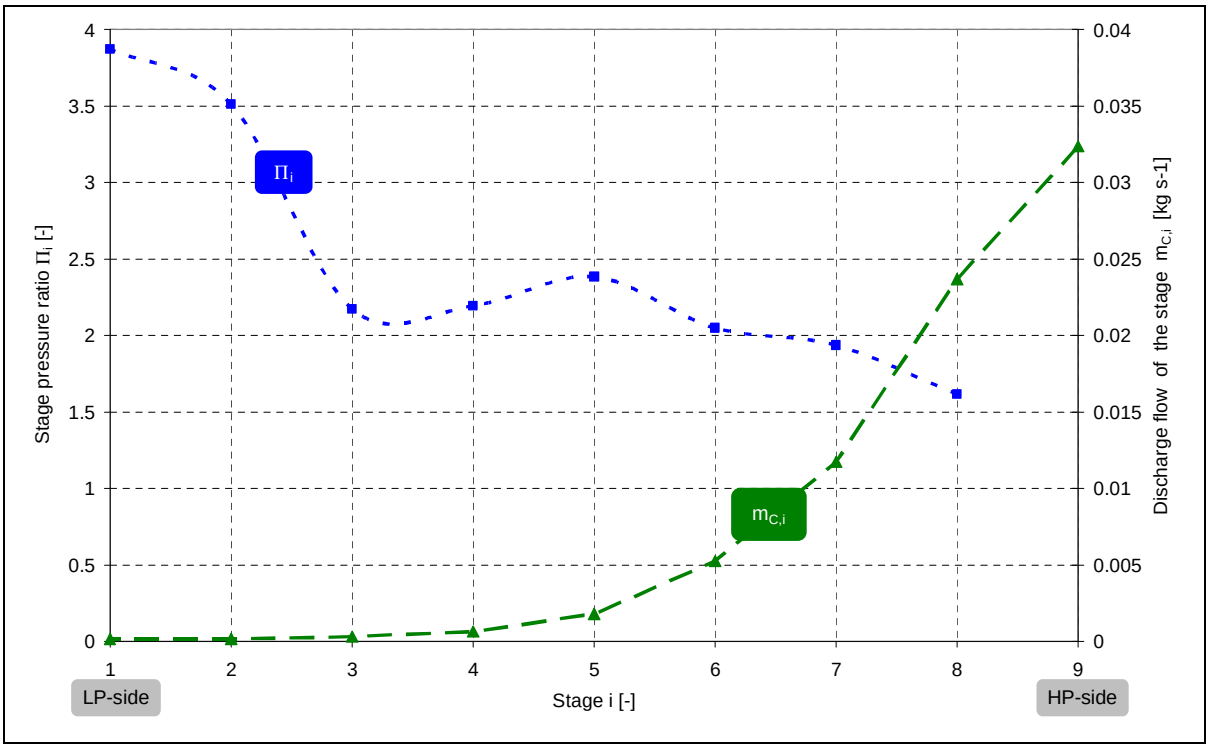

Fig. 6 Stage pressure ratios and mass flows along the rotor stages for the rotor optimized with regard to the specific internal work (Fig. 4)

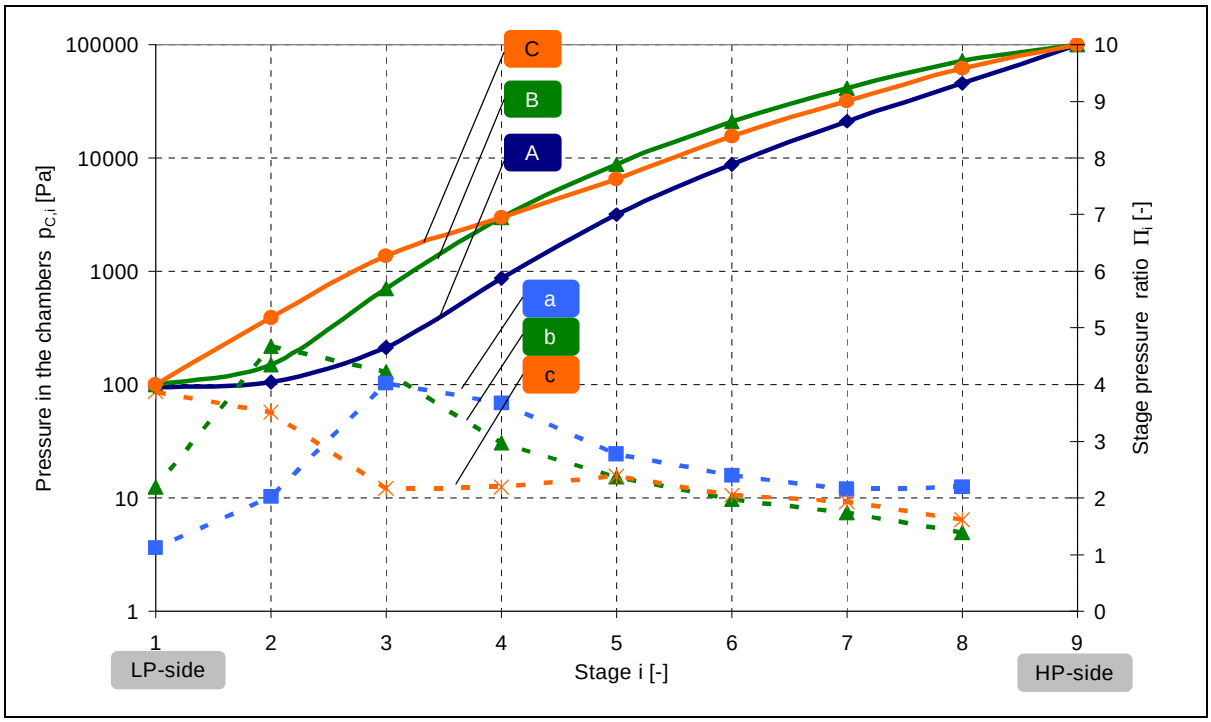

Fig. 7 Pressure curve and stage pressure ratio over the rotor stages

A: Pressure curve of the isochoric rotor
B: Pressure curve of the rotor with linear pitch variation
C: Pressure curve of the optimized rotor
a: Stage pressure ratio of the isochoric rotor
b: Stage pressure ratio with linear pitch variation
c: Stage pressure ratio of the optimized rotor

The discharge mass flow of the stage increases towards the pressure side – due to the increasing density of the working medium. Fig. 7 shows a comparison of the calculated

pressure in the stages and the stage pressure ratio between a rotor with constant working chamber volume per stage, a rotor with linear pitch variation and the rotor with optimized pitch.

Considering the pressure curve of the isochoric rotor geometry (a), the pressure ratio in stage 3 takes the maximum value. A comparison with the pressure profile of the linear pitch variation (b) shows that the main portion of the pressure ratio is further shifted towards the LP-side. The optimized rotor (c) reaches the maximal stage pressure ratio in the area of the sucking stage, followed by a decline of the pressure ratios towards the high-pressure side.

Fig. 8 shows a comparison of the internal power resulting from the stage pressure ratios and the respective discharge mass flows, referring to the discharged mass flow.

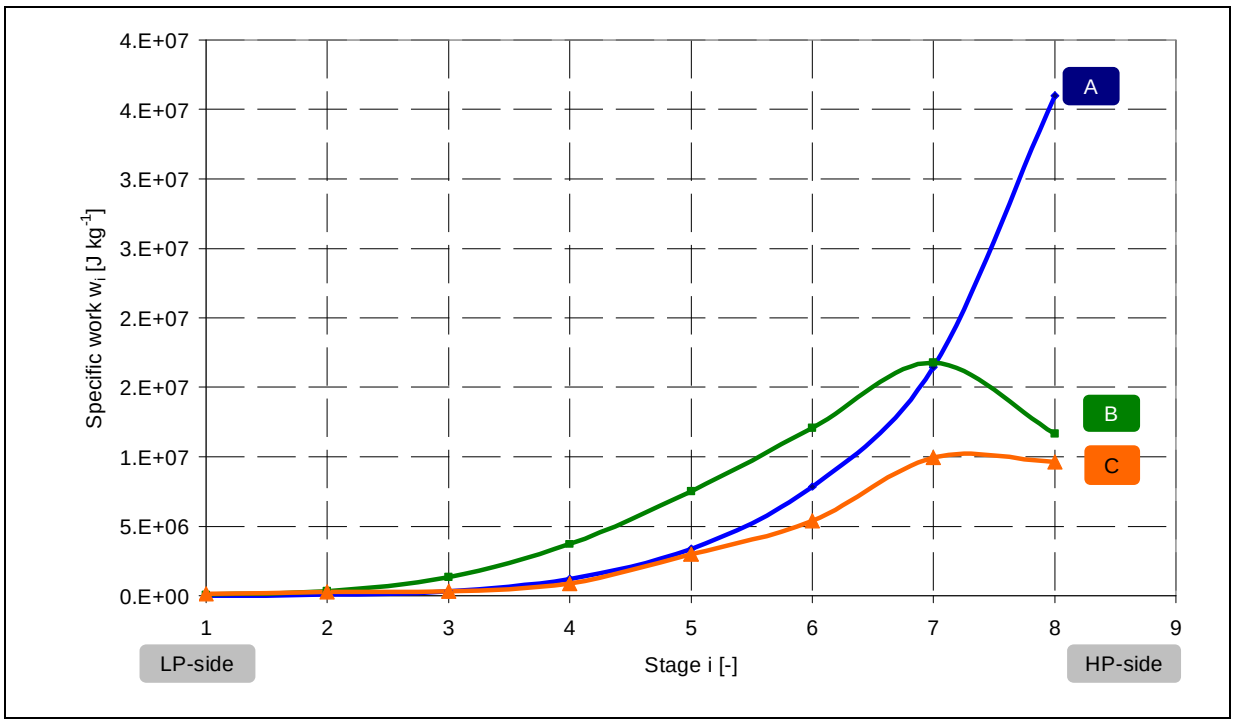

Fig. 8 Curve of the specific internal work per stage w_i referring to the sucked mass flow, plotted over the rotor stages

A: Isochoric rotor
B: Rotor with linear pitch variation
C: Optimized rotor

Above all in the area of the working chamber on the high-pressure side, the optimized rotor (c) attains a significant reduction of the specific stage power compared to the isochoric rotor (a) and the rotor with linear pitch variation (b). The physical reasons are to be found in the relationship between the stage pressure ratio and the gap mass flow of the stages predominantly resulting from the density.

5 Summary and outlook

In a simplified example, which considers only the gap mass flow through the housing gap, the relationship between the working chamber volumes, the stage pressure ratios and the

isentropic compression work for different suction pressures are illustrated. The analysis shows that it is possible to attain a minimum of specific work with the variation of the chamber volumes at constant total volume.

The expansion of the number of stages and the inclusion of further gap connections as well as the application of evolutionary algorithms enable the subsequent calculation of the pitch curve, optimized with regard to the specific internal work, for a screw-type vacuum pump with 8 stages. The comparison with a rotor showing a linear pitch variation confirms a clear reduction of the specific work.

The experimental verification of the optimization results is planned within the framework of the upcoming experimental surveys in the chair of fluidics.

6 List of symbols used

Symbol	Meaning	Dimension
A	Area	m^2
Cp	Specific heat capacity	$J\ kg^{-1}\ K^{-1}$
$\dot{m}$	Mass flow	$kg\ s^{-1}$
n	Rotary speed	min^{-1}
p	Pressure	Pa
P	Internal power	W
V	Volume	m^3
$\dot{V}$	Volume flow	$m^3\ s^{-1}$
R	Specific gas constant	$J\ kg^{-1}\ K^{-1}$
s	Pitch	m
w	Internal work	J
α	Orifice coefficient for gap mass flows	-
k	Isentropic exponent	-
Π	Pressure ratio	-

C	Working chamber
F	Femal rotor
G	Gap
HP	High-pressure „side“
i	Stage index
LP	Low-pressure “side“
M	Male Rotor

7 Literature

[1] Wutz, ET AL. Handbuch Vakuumtechnik. Theorie und Praxis, 7th extended version Vieweg, Braunschweig Wiesbaden, 2000

[2] Patent DE 602 16 089. A, MATSUBARA KATSUMI, UCHIDA RIICHI, MATSUBARA MASATOSHI, SCREW VACUUM PUMP, 11.04.84

[3] PATENT DE 695 23 959. OZAKI, MASAYUKI ; AKUTSU, ISAO , Schraubenkolbenmaschine, 19.08.1995

[4] Wenderott, D. Spaltströmungen im Vakuum, dissertation, University of Dortmund, VDI Progress Reports, serial 7, Nr.423, VDI-Verlag, Düsseldorf, 2001

[5] Rohe, A. ROHE, A.: Wärmehaushalt von Schraubenspindel-Vakuumpumpen. dissertation , University of Dortmund 2005,

[6] Kauder, K. Rohe, A. Simulation und Messung des Druckverlaufes am Beispiel einer Schraubenspindel – Vakuumpumpe, Schraubenmaschinen No. 10, p. 137-148, University of Dortmund, 2002

[7] Helpertz, M. Methode zur stochastischen Optimierung von Schraubenrotorprofilen. Dissertation, University of Dortmund 2003